

# Electronic structure of van der Waals magnetic semimetal GdGaI

Kohei Yamagami, Ryotaro Okuma, Yoshinari Okada

Okinawa Institute of Science and Technology Graduate University, Tancha, Onna-son, Kunigami-gun  
Okinawa, 904-0495, Japan.

Recently, we have succeeded to grow relatively large size van der Waals (vdW) magnetic semimetal GdGaI (GGI). The crystal structure and picture of GdGaI is shown in **Fig. 1a**. The density functional theory (DFT) based band calculation for GGI suggests semi-metallic electronic structure. The DFT band structure is analogous to that of TiSe<sub>2</sub>, which is known as a 2D material hosting charge density wave (CDW) and/or exciton formation [1]. Compared to non-magnetic TiSe<sub>2</sub>, emergence of weak ferromagnetism at low temperature is an interesting unique characteristic in GGI. While rich deformation of band structure is naturally expected, experimental report on electronic structure in GGI has been lacking so far.

Here, we report angle resolved photoemission spectroscopy (ARPES) on GGI. **Fig. 1b** shows ARPES dispersion around  $\Gamma$  point, using 7 eV laser with p-polarization [2]. For comparison, ARPES dispersion using He discharge lamp is also shown in **Fig. 1c**. Below  $E-E_F=-0.4$  (eV), two bands are clearly visualized in laser ARPES data (**Fig. 1b**). Above  $E-E_F=-0.4$  (eV), the hole bands around the  $\Gamma$  point were similarly observed in both cases. The band top of the hole band is around  $E-E_F\sim-0.18$  (eV), which reflects band gap opening by  $2a \times 2a$  ordering. The clear difference between two ARPES dispersion (**Fig. 1b and c**) is near  $E_F$  intensity distribution in  $k$  space. This presumably suggests the importance of understanding characteristic spin and orbital nature in near  $E_F$  hole band, together with prominent spin-orbital coupling effect in this system.

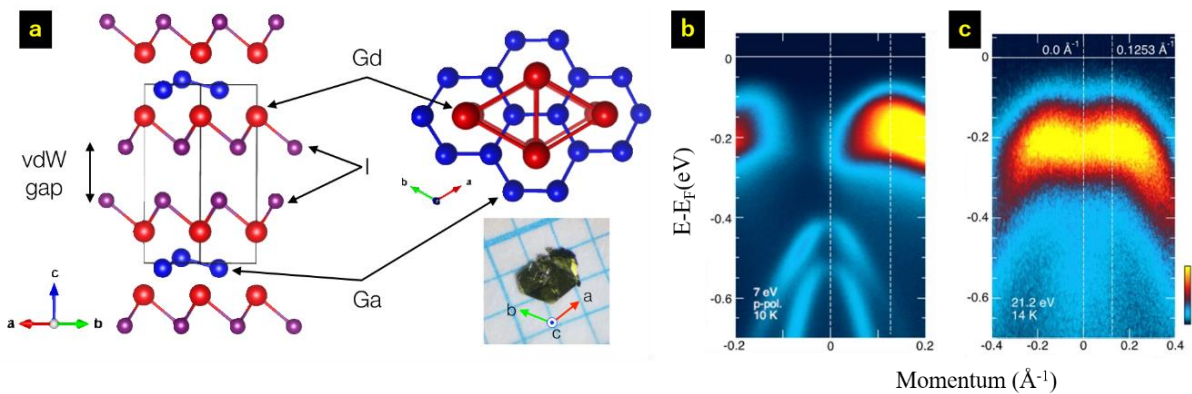


**Figure 1.** (a) The crystal structure and picture of GdGaI. (b)(c) The angle resolved photoemission spectroscopy (ARPES) data around  $\Gamma$  point, using (b) He discharge lamp and (c) 7 eV laser. The measured temperature for (b) and (c) are 10K and 14K, respectively. In (b), p-polarization is used.

## References

- [1] H. Cercellier, *et al.* Phys. Rev. Lett. **99**, 146403 (2007).
- [2] K. Yaji *et al.*, Rev. Sci. Instrum. **87**, 053111 (2016).

# ENHANCEMENT OF RASHBA SPLITTING IN SNPC/AU(111)

Kaname Kanai

*Department of Physics, Faculty of Science and Technology, Tokyo University of Science*

The growth of sub-monolayers of tin phthalocyanine (SnPc) molecules on Au(111) has been confirmed by angle-resolved photoemission spectroscopy (ARPES) to enhance the energy band splitting due to the Rashba spin-orbit interaction appearing in the Shockley state (SS). This result provides knowledge for understanding the electronic structure of Rashba-type SS at the interface between organic molecules and metal substrates.

The electronic structure of the interface between a metal surface and molecules adsorbed on that surface has been a long-standing issue in surface science. Recently, this issue has attracted more attention due to its importance in organic semiconductor devices. The electronic structure of an interface at an electrode metal surface covered with organic semiconductor molecules (organic/metal interface) is directly responsible for the electronic properties of the device because the relationship between the molecular orbital energies and the Fermi level of the metal at the interface determines the carrier injection barrier from the electrodes into the semiconducting layers. Thus, in order to realize a device with high carrier injection efficiency, it is vital to understand the formation of the electronic structure at the organic/metal interface.

SS is a characteristic electronic state peculiar to the crystal surface. By breaking the spatial inversion symmetry of the crystal in the normal direction to the surface, a free electron-like parabolic dispersion appears near the surface. In particular, it is known that in noble metal crystals such as copper, silver, and gold, large spin-orbit coupling can cause Rashba effects of practically observable magnitude to appear. The Rashba effect lifts the spin degeneracy of the SS band dispersion and splits it into two parabolas that are completely spin-polarized except at the  $\Gamma$  point. Recently, it has been reported that this Rashba effect is enhanced at metal interfaces such as Bi/Ag(111) [1], TTC/Au(111) [2], and rare gas atoms/Au(111) interfaces. Attempts have also been made to create devices that can convert spin currents to spin currents by generating the Edelstein effect at the molecule/metal interface using the giant Rashba effect [3,4]. Therefore, understanding the mechanism by which molecular adsorption significantly affects the Rashba effect is not only of interest in surface science, but should provide fundamental information for future spintronics. In this study, we aimed to directly observe in detail the influence of tin-phthalocyanine (SnPc) molecules, a typical organic semiconductor molecule, on the Rashba effect that appears in SS of Au(111).

The single crystal of Au(111) sample was used for the substrate. Before vapor deposition of SnPc on it, the surface of this Au(111) substrate was cleaned in UHV by sputter-anneal cycles. Anneal temperature was 773 K. This clean surface was evaluated by low energy electron diffraction (LEED) measurement. After outgassing, SnPc was deposited on Au(111) at normal incidence from resistively heated Knudsen cell. The deposition rate of 0.0005 ~ 0.002 nm/s was measured with a quartz crystal microbalance oscillator. The deposition of SnPc on Au(111) was carried out in a stepwise manner: the SnPc film thickness were 0.06, 0.13, 0.19, and 0.26 ML. The electronic structure of SnPc/Au(111) was measured by ARPES at 28 K.

When SnPc thin film is grown on Au(111), the SS rapidly disappears as the coverage increases. This is probably due to the loss of translational symmetry in the direction parallel to the surface, caused by the random orientation of the molecules on the surface. This hypothesis can be easily inferred from the three-dimensional molecular structure of SnPc, which is called “shuttlecock” as shown in Fig. 1. However, when the coverage of the grown SnPc thin film is very low, SnPc appears to grow epitaxially on Au(111), and

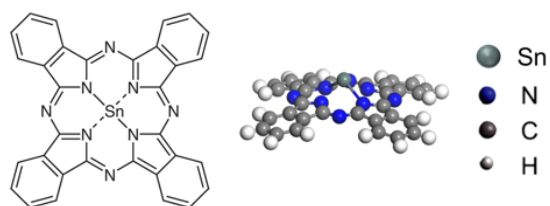


Fig. 1. Molecular structure of SnPc (left). Three-dimensional structure of SnPc (right).

the Au(111) SS does not disappear. Furthermore, it was observed that the Au(111) SS was greatly affected by molecular adsorption.

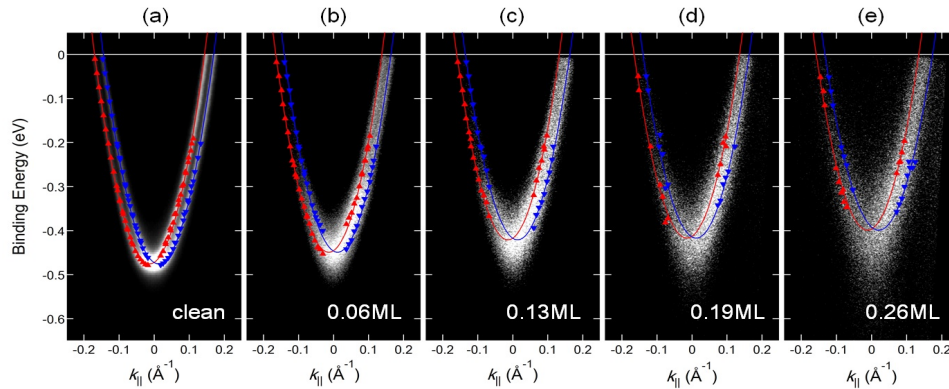


Fig. 2. The thickness dependence of SnPc/Au(111) Rashba-type SS measured at 28 K using ARPES. The results of (a) Au(111) clean surface, (b) SnPc 0.06ML/Au(111), (c) SnPc 0.13ML/Au(111), (d) SnPc 0.26ML/Au(111), and (e) SnPc 0.32ML/Au(111). The red or blue plots on the data are the results of peak fitting analysis at EDC (Energy Distribution Curve) and MDC (Momentum Distribution Curve) maps.

Fig. 2 shows the ARPES spectra ( $h\nu = 6.998$  eV) of SnPc/Au(111). It can be seen that SS in Au(111) is modified as the coverage of SnPc increases. Energy of SS in Au(111) was significantly lowered with increasing the PbPc thickness. However, SS was observable only in the case of very low coverage of SnPc, and SS disappeared before the coverage of one molecular layer was reached.

Fig. 3 shows thickness dependence of Rashba parameter  $\alpha_R$  and Rashba splitting  $\Delta k_{\parallel}$  calculated by EDC and MDC analysis of the ARPES results in Fig. 2. As the value of  $\Delta k_{\parallel}$  increased, the value of  $\alpha_R$  also tended to increase as the film thickness increased.

In conclusion, we observed the enhancement of Rashba effect by adsorption SnPc thin film on Au(111). One possible factor that enhances the Rashba effect at the SnPc/Au (111) interface is due to the potential gradient caused by the adsorption of molecules with evenly aligned dipole directions, which is needed to be further verified in the future. The results presented here allowed us to discuss the interfacial electronic states formed by adsorbed metallic phthalocyanines, in relation to their effect on the Rashba effect.

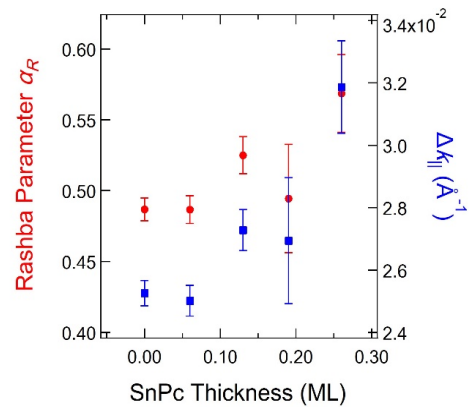


Fig. 3. Thickness dependence of Rashba parameter  $\alpha_R$  and  $\Delta k_{\parallel}$  calculated from SnPc/Au(111) Rashba-type SS observed by ARPES.

## REFERENCES

- [1] C. R. Ast, J. Henk, A. Ernst, L. Moreschini, M. C. Falub, D. Pacil , P. Bruno, K. Kern and M. Gironi, *Phys. Rev. Lett.* **98**, 186807 (2007).
- [2] H. Mizushima, H. Koike, K. Kuroda, Y. Ishida, M. Nakayama, K. Mase, T. Kondo, S. Shin and K. Kanai, *Phys. Chem. Chem. Phys.*, **19**, 18646 (2017).
- [3] S. Takizawa, K. Kondou, H. Isshiki, K. Shimose, T. Kawabe, S. Miwa and Y. Otani, *IEEE Trans. Magn.*, **54**, 11 (2018).
- [4] H. Isshiki, K. Kondou, S. Takizawa, K. Shimose, T. Kawabe, E. Minamitani, N. Yamaguchi, F. Ishii, A. Shiotari, Y. Sugimoto, S. Miwa and Y. Otani, *Nano Lett.*, **19**, 7119 (2019).

# SARPES STUDY OF A NEW WEYL SEMIMETAL OF THE CDW COMPOUNDS

Chun Lin<sup>1</sup>, Kenta Kuroda<sup>1</sup>, Ryo Noguchi<sup>1</sup>, Kaishu Kawaguchi<sup>1</sup>, Ayumi Harasawa<sup>1</sup>, Shik Shin<sup>2</sup>, Masanobu Miyata<sup>3</sup>, Koyano Mikio<sup>3</sup>, and Takeshi Kondo<sup>1,4</sup>

<sup>1</sup>*The Institute for Solid State Physics, The University of Tokyo*

<sup>2</sup>*Office of University Professor, The University of Tokyo*

<sup>3</sup>*School of Materials Science, Japan Advanced Institute of Science and Technology*

<sup>4</sup>*Trans-scale Quantum Science Institute, The University of Tokyo*

The emergent quantum phenomena in low dimensional materials have attracted increasingly more attention in the realm of not only fundamental science but also practical applications. These compounds typically host multiple broken symmetry orders such as charge density wave (CDW), superconductivity, and other magnetism- and spin-related exotic quantum phenomena [1], providing a multifunctional platform for investigations of basic physics and real-world applications owing to their low dimensionality suitable for engineering. On the other hand, topological semimetal is a new class of quantum matters with characteristic topological surface states originated from the topology of their bulk band structure [2]. In particular, the Weyl semimetal is a condensed-matter realization of Weyl fermions manifested as low-energy excitations, in which band dispersions exhibit linear crossings at pairs of Weyl points, with either broken spatial inversion or time-reversal symmetry.

Ta<sub>2</sub>Se<sub>8</sub>I is well known as a prototypical quasi-one-dimension (quasi-1D) CDW system stacked by TaSe<sub>4</sub> chains along the *c* axis with body center tetragonal lattice (Figs. 1a,b). The CDW sets in at a temperature around 260 K revealed by resistivity [3] as shown in Fig. 1d [4]. The CDW wave vector was confirmed by X-ray diffraction to be ( $\pm 0.045$   $2\pi/a$ ,  $\pm 0.045$   $2\pi/b$ ,  $\pm 0.085$   $2\pi/c$ ) [5]. Nevertheless, a long-standing puzzle remains in that the energy gap is much larger than the mean-field value and it refrains from closing at temperatures far above the CDW onset, as confirmed by, e.g., optical spectra [6] and angle-resolved photoemission spectroscopy (ARPES) [7,8]. Such an anomalous behavior was attributed either to a fluctuating CDW in an extreme 1D manifestation [6] or the formation of small polarons dressing mobile electrons owing to strong electron-phonon coupling [7,8]. Recently, first principle calculations indicate that the high-temperature phase of this compound is actually a Weyl semimetal [9], from which the transport signals of chiral anomaly have been successfully captured in the CDW state [4]. Ta<sub>2</sub>Se<sub>8</sub>I, therefore, offers a very rare realization of strong correlation driven topological phase transition [9].

Here, we present laser-based spin-resolved ARPES (at Institute for Solid State Physics, the University of Tokyo) results in the distorted phase of this newly predicted Weyl semimetal and provide evidence of spin-polarized Weyl cone whose experimental observation remains challenging in the literature.

Figure 1g shows the constant-energy contour map at a binding energy of 0.6 eV acquired at 100 K with 7 eV laser and on the (110) surface of conventional cell which is easily cleaved due to the weak van der Waals interactions among quasi-1D chains. The bulk Brillouin zone and its surface projection (reddish shaded) are shown in Fig. 1c. One can see that the band structure features a wiggle perpendicular to the chain direction indicative of a finite interchain interaction, which is consistent with synchrotron-ARPES [7,8]. In Figs. 1h,i, we present the dispersions along two momentum cuts crossing the Weyl points, as indicated in Fig. 1g with corresponding colored arrows. A spectral suppression manifested as a 0.2 eV energy gap agrees with the polaron scenario [7]. Below this polaron gap, the band disperses in a linear Dirac-like manner as indicated by the red lines in Figs. 1h,i, consistent with the proposed

electronic structure of a Weyl semimetal (Fig. 1e [9]). Taking advantage of spin resolution, we obtained the energy distribution curves of spin-up and spin-down states at a momentum point of the (purple arrow in Fig. 1i), as shown in Fig. 1j. The resulting spin polarization (green curve in Fig. 1j) suggests a spin-polarized Weyl cone in the CDW state.

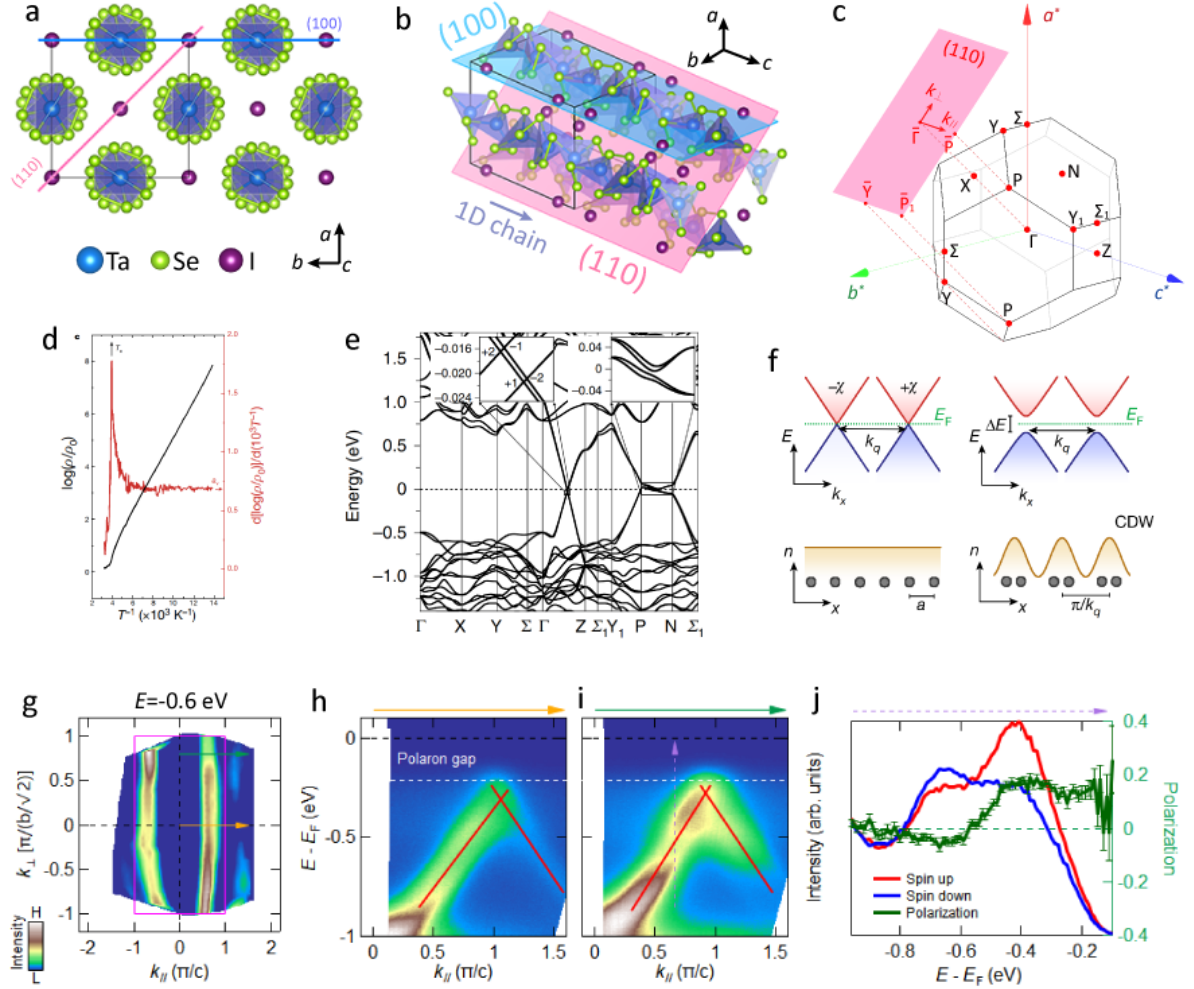


**Fig. 1** **a,b**, Crystal structure of  $\text{Ta}_2\text{Se}_3\text{I}$ . **c**, Bulk Brillouin zone and its projection onto conventional (110) surface. **d**, Characteristic resistivity showing a CDW transition around 260 K [4]. **e**, Band structure along high-symmetry lines calculated from density functional theory with spin-orbit coupling [9]. **f**, Schematic of a CDW gapped Weyl semimetal [4]. **g-i**, Our preliminary data of constant-energy contour ( $E_B = 0.6$  eV) and band dispersions along two momentum cuts indicated by the corresponding colors. Small polarons dress photoelectrons featured by a polaron gap as indicated. Red lines in **h,i** are guides for the eyes. **j**, Our preliminary data of spin-resolved energy distribution curves and spin polarization along the dashed purple arrow indicated in **i**.

## REFERENCES

- [1] P. Monceau, *Advances in Physics* **61**, 325 (2012)
- [2] N. P. Armitage *et al.*, *Rev. Mod. Phys.* **90**, 015001 (2018)
- [3] Z. Z. Wang *et al.*, *Solid State Commun.* **46**, 325–328 (1983)
- [4] J. Gooth *et al.*, *Nature* **575**, 315–319 (2019)
- [5] H. Fujishita *et al.*, *Solid State Commun.* **49**, 313–316 (1984)
- [6] H. P. Geserich *et al.*, *Physica B+C* **143**, 198–200 (1986)
- [7] L. Perfetti *et al.*, *Phys. Rev. Lett.* **87**, 216404 (2001)
- [8] C. Tournier-Colletta *et al.*, *Phys. Rev. Lett.* **110**, 236401 (2013)
- [9] W. Shi *et al.*, *Nature Physics* **17**, 381–387 (2021)

# OBSERVATION AND CONTROL OF THE WEAK TOPOLOGICAL INSULATOR STATE IN ZRTE<sub>5</sub>

Peng Zhang<sup>1</sup>, Ryo Noguchi<sup>1</sup>, Kenta Kuroda<sup>1</sup>, Chun Lin<sup>1</sup>, Kaishu Kawaguchi<sup>1</sup>, Koichiro Yaji<sup>2</sup>, Ayumi Harasawa<sup>1</sup>, Mikk Lippmaa<sup>1</sup>, Simin Nie<sup>3</sup>, Hongming Weng<sup>4</sup>, V. Kandyba<sup>5</sup>, A. Giampietri<sup>5</sup>, A. Barinov<sup>5</sup>, Qiang Li<sup>6</sup>, G. D. Gu<sup>6</sup>, Shik Shin<sup>1</sup>, Takeshi Kondo<sup>1</sup>

<sup>1</sup>Institute for Solid State Physics, University of Tokyo

<sup>2</sup>Research Center for Advanced Measurement and Characterization, NIMS

<sup>3</sup>Department of Materials Science and Engineering, Stanford University

<sup>4</sup>Institute of Physics, Chinese Academy of Sciences

<sup>5</sup>Elettra - Sincrotrone Trieste

<sup>6</sup>Condensed Matter Physics and Materials Science Department, Brookhaven National Laboratory

A quantum spin Hall insulator hosts topologically protected edge states, in which backscattering by nonmagnetic impurities is prohibited and dissipationless current is possible. Its 3D analogue, a weak topological insulator (WTI), possesses surface states at the ‘side’ surface that are not weak, but as robust as the wide-studied strong topological insulators, and there may be even less scattering channels due to the highly directional surface electrons [1]. However, since the topological states only appear on side surfaces, it is difficult to prepare such a clean surface and to study the WTI states. Here, we report for the first time the visualization of the topological surface states of the WTI candidate ZrTe<sub>5</sub>. A quasi-1D spin-momentum locked band on the side surface was distinguished. Furthermore, control of the band gap by external strain was confirmed directly by ARPES: a WTI state with a larger gap and a topological phase transition to an ideal Dirac semimetal state are realized.

## Topological surface states observed on the side surface

ZrTe<sub>5</sub> was predicted to be a WTI candidate at the early stage of exploring WTIs [2], in which there is no surface state on the top surface, while on the side surface there is topological surface state, as shown in Fig. 1(a). It has a quasi-1D crystal structure. Along the lattice *b* direction, the layers are stacked by van der Waals forces, and a clean surface can be easily obtained by cleavage. Instead, Te–Te bonding exists between adjacent layers along the lattice *c* direction, causing much more difficulty in cleaving the side *a*-*b* surface. Due to the difficulty to cleave the side surface, all the previous surface-sensitive studies were carried out

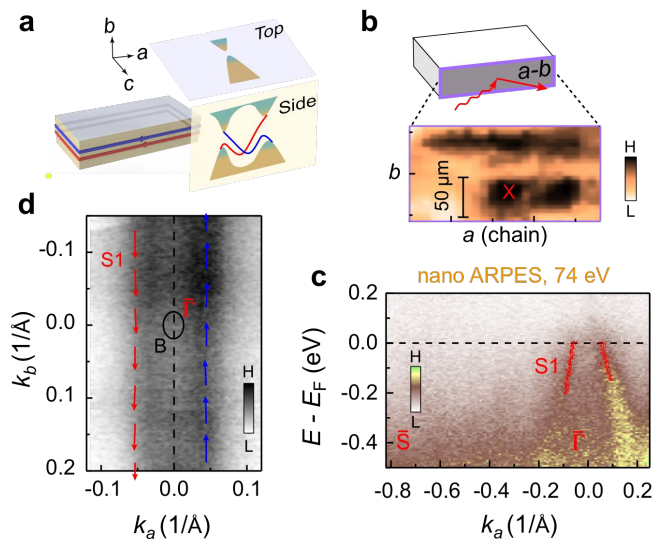


**Figure 1 ARPES measurement on the side surface of ZrTe<sub>5</sub>.** (a) Band structure of a WTI on the top surface and side surface. (b) Intensity mapping in the real space for the cleaved area of the side surface from a nano-ARPES. (c) Band structure measured at the position indicated by red cross in (b). (d) Fermi surface measured with laser ARPES. The red and blue arrows indicated the spin direction measured with a spin-resolved ARPES.

on the top surface. Whether or not this material is topological, which relies on the measurement from side surface, has not been determined beyond speculation. We successfully prepared the side surface of this sample [3]. With a synchrotron-based nano-ARPES (spot size  $< 1 \mu\text{m}$ ), we took real space maps of photoemission intensity on several samples, as sketched in Fig. 1(b). It is found that the typical dimension of cleaved areas is around or smaller than  $50 \mu\text{m}$ . Along lattice  $a$  direction, the band shows a hole-like dispersion (Fig. 1(c)). In  $k$ -space, a quasi-1D Fermi surface is exhibited by plotting ARPES intensities about the Fermi level, which shows no dispersion along lattice  $b$  direction (Fig. 1(d)). We further observed a clear spin polarization along lattice  $b$  direction. In contrast, the spin polarization is almost zero along the lattice  $a$  and  $c$  directions, as sketched by red and blue arrows in Fig. 1(d). Therefore, the band is spin-polarized along the  $b$ -direction with spin-momentum locking, consistent with the spin-texture of WTIs with a quasi-1D dispersion.

### Strain-tuned topological phase transition observed on the top surface

First-principles calculations predict that  $\text{ZrTe}_5$  is close to a topological phase transition, which may be tuned by external strain. We used a strain device shown in Fig. 2(a) to apply both compressive and tensile strain. On the top surface, without strain we observed a small bulk gap ( $\sim 28 \text{ meV}$ ), as shown in the middle panel of Fig. 2(b). The small bulk gap indicates that the WTI state in  $\text{ZrTe}_5$  is protected only marginally from external perturbations. With tensile strain, the band gap is enlarged to  $\sim 51 \text{ meV}$ . In contrast, we could reduce the band gap by compressive strain, even realizing a Dirac semimetal state with no band gap. The corresponding first-principles calculations are displayed in Fig. 2(c), which is consistent with the experimental results. In Fig. 2(d), we summarized the topological phase diagram of  $\text{ZrTe}_5$ .

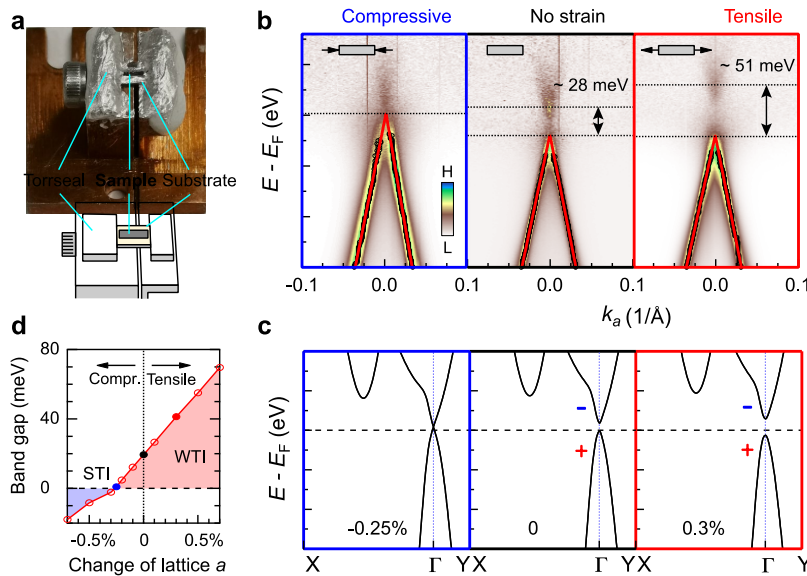


**Figure 2 Strain-tuned topological phase transition in  $\text{ZrTe}_5$ .** (a) Strain device we used to apply both compressive and tensile strain. (b) Band structure measured from top surface with both compressive and tensile strain. (c) Corresponding band structures from first-principles calculations. (d) Phase diagram of  $\text{ZrTe}_5$  with different strain.

### References:

- [1] R. Noguchi et al., Nature, 566, 518 (2019).
- [2] H. Weng, X. Dai & Z. Fang, Phys. Rev. X 4, 011002 (2014).
- [3] P. Zhang et al., Nature Commun. 12, 406 (2021).

# ANGLE-RESOLVED PHOTOEMISSION SPECTROSCOPY OF GALLIUM SINGLE CRYSTAL SURFACE

Koichiro Yaji<sup>1</sup>, Kenta Kuroda<sup>2</sup>, Fumio Komori<sup>2</sup>

<sup>1</sup>Research Center for Advanced Measurement and Characterization,  
National Institute for Material Science

<sup>2</sup>Institute for Solid State Physics, The University of Tokyo

Topological insulators have been intensively studied in last decade, where the spin-polarized surface states on the topological insulators can be understood with the topology of the wavefunctions of an electron. A concept common to the topological insulator is applicable to the superconductor, so-called a topological superconductor. The topological superconductor is predicted that the surface states host the emergence of Majorana bound states. Recently, we revealed that an iron-based superconductor FeSe<sub>0.55</sub>Te<sub>0.45</sub> is the topological superconductor [1]. Here, it is important to clarify the Fermi surface and the energy band dispersion to identify if the material is the topological superconductor.

An elemental gallium is a pure metal. The bulk gallium crystals have a rich phase diagram. Among them, only the orthorhombic phase, so-called  $\alpha$ -gallium ( $\alpha$ -Ga), is stable at atmospheric pressure. The  $\alpha$ -Ga exhibits giant magnetoresistance though that is a non-magnetic material, which can be originating from topological property [2]. Moreover, the superconductivity was confirmed by both specific heat and resistivity measurements [2]. Therefore, the  $\alpha$ -Ga would offer an interesting platform for understanding coexistence of non-trivial electronic states and superconductivity in the pure metal. In our previous study using synchrotron radiation, we have clearly observed the surface state of  $\alpha$ -Ga. The aim of the present study is the investigation of the spin structure of the surface states with spin-resolved ARPES.

The  $\alpha$ -Ga single crystal was prepared from super-cooled Ga [2]. Due to the low melting temperature, the special care was needed when we treated the crystal during polishing and *in situ* cleaning procedures. The  $\alpha$ -Ga(010) surface was mechanically polished using diamond paste. Subsequently, the surface was then cleaned by repeated cycles of 0.7 keV Ne<sup>+</sup> sputtering at 273 K and annealing up to 273 K in the ultra-high vacuum chamber. The clean surface was checked by low energy electron diffraction (LEED).

Figure 1 shows a LEED pattern from  $\alpha$ -Ga(010) at 0 °C. We find sharp LEED spots, indicating that a high-quality single crystal surface has been obtained. Here, the  $\alpha$ -Ga(010) surface has a glide plane in [100] direction. Thus, the odd-number spots in the [100] direction disappear, which is in good agreement with former study [4].

The ARPES measurements were performed at E-building in ISSP. Photoelectrons were excited by a 7-eV laser light. The sample temperature was kept at 35 K during the measurements. However, unfortunately, photoelectron intensity with 7-eV photons was not enough to observe the band of  $\alpha$ -Ga(010) due to the low photoionization cross section.

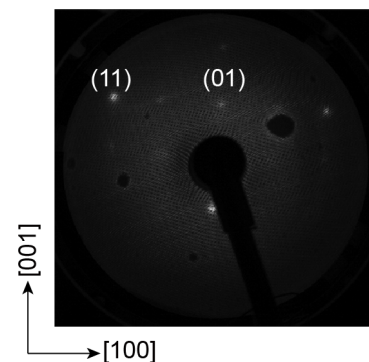


Fig. 1. LEED pattern of  $\alpha$ -Ga(010) with the primary energy of 31 eV at 273 K.

## REFERENCES

- [1] P. Zhang *et al.*, Science **360**, 182 (2018).
- [2] B. Chen *et al.*, npj Quantum Materials **3**, 40 (2018).
- [3] K. Yaji *et al.*, Rev. Sci. Instrum. **87**, 053111 (2016).
- [4] Ch. Søndergaard *et al.*, Phys. Rev. B **67**, 205105 (2003).



# STUDY ON THE SPIN TEXTURE OF THE TOPOLOGICAL STATES IN QUASI-ONE-DIMENSIONAL MATERIAL

Deyang Wang<sup>1</sup>, Mao Ye<sup>1</sup>, Kenta Kuroda<sup>2</sup>, Koichiro Yaji<sup>2</sup>, Ayumi Harasawa<sup>2</sup>, Takeshi Kondo<sup>2</sup>  
<sup>1</sup>*State Key Laboratory of Functional Materials for Informatics, Shanghai Institute of Microsystem and Information Technology, Chinese Academy of Science, Shanghai 200050, People's Republic of China*

<sup>2</sup>*Institute for Solid State Physics, The University of Tokyo, Kashiwa, Chiba 277-8581, Japan.*

The reducing of dimensionality in materials significantly increases electrons' anisotropy. This is especially important for topological materials, where the backscattering is prohibited due to the protection of time-reversal-symmetry. For quasi-one-dimensional (quasi-1D) materials, the occurrence of scattering is even more strictly prohibited than that in materials with higher dimensionality, because quasi-1D materials only possess one dimensional conductive channel. Therefore, the topological states in quasi-1D materials are considered to be a promising platform for the development and application of spintronics devices with low energy consumption.

TaNiTe<sub>5</sub> is predicted to be a candidate for quasi-1D topological materials, in which the highly anisotropic transport properties and nontrivial Berry phases have been confirmed<sup>[1]</sup>. However, the direct experimental observation of the topological surface states in TaNiTe<sub>5</sub> are still missing. Thus, the band topology in this quasi-1D materials remains unclear. In this study, we unambiguously reveal the topological surface states in TaNiTe<sub>5</sub> by means of high resolution laser spin- and angle-resolved photoemission spectroscopy (laser-SARPES) combined with DFT calculations.

High quality single crystalline TaNiTe<sub>5</sub> samples were grown by self-flux method, and then characterized by the X-ray Diffraction and Energy Dispersive Spectroscopy. The high-resolution laser- SARPES experiments were conducted at the Institute for Solid State Physics, University of Tokyo, equipped with 6.994 eV photons laser and ScientaOmicron DA30L analyzer<sup>[2]</sup>. The density functional theory (DFT) calculations were performed via *Vienna ab initio Simulation Package*<sup>[3]</sup> for bulk bands and WannierTools<sup>[4]</sup> for surface states.

The crystal structure of TaNiTe<sub>5</sub> is shown in Figure 1(a), where the NiTe<sub>2</sub> quasi-1D atomic chains extend along *a* direction. The Van der Waals layers stack along *b* direction, where the crystal can be easily cleaved. Figure 1(b) shows the corresponding bulk Brillouin zone (BZ) and surface projected BZ for the cleaved plane. The Fermi surface measured by laser-ARPES is shown in Figure 1(c), showing strong anisotropic properties, which shows good agreement with the calculated Fermi surface obtained by DFT method as shown in Figure 1 (d). Figure 1 (e) shows the spin-resolved band structure along  $\bar{Z}-\bar{\Gamma}-\bar{Z}$  direction. Two sets of Dirac-type surface bands (denoted as  $\alpha$  and  $\beta$ ) near the Fermi energy, and one set of Rashba-type bands (denoted as  $\gamma$ ) located at binding energy around 0.4 eV are clearly resolved. The spin-resolved results reveal that both  $\alpha$  and  $\beta$  bands possess spin-momentum-locking spin texture, and are well reproduced by our DFT calculations [Figure 1(f)], indicating the existence of topologically non-trivial surface states.

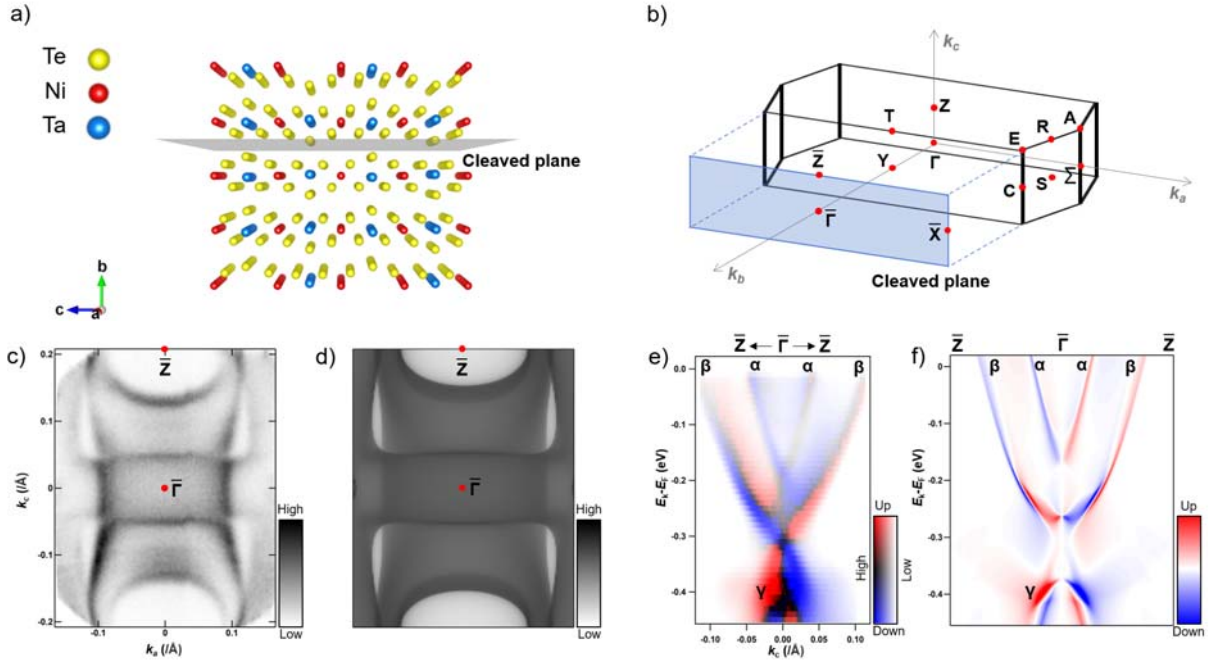


Figure 1 (a) Crystal structure and cleaved plane of TaNiTe<sub>5</sub>. (b) Three-dimensional (3D) bulk Brillouin zone (BZ) and the projected surface BZ for cleaved plane. (c) Spin-integrated Fermi surface intensity measured by 7-eV laser-ARPES. (d) Fermi surface obtained by DFT calculations. (e) Spin-resolved band structure along  $\bar{Z}-\bar{\Gamma}-\bar{Z}$  direction measured by spin-ARPES, while red and blue stands for spin-up and spin-down in  $k_a$  direction, black and white represents the intensity distribution. (f) Spin-resolved band structure along  $\bar{Z}-\bar{\Gamma}-\bar{Z}$  direction obtained by DFT calculations.

In summary, we observed the surface states and its spin-texture of the quasi-1D material TaNiTe<sub>5</sub> through high-resolution laser-ARPES experiments, and further confirmed by the comparison with DFT calculations. Further examination of the band topology, as well as the experimental measurements on other cleaved planes would benefit the determination of the topological properties in the quasi-1D TaNiTe<sub>5</sub> materials.

## REFERENCES

- [1] Xu, Chunqiang, et al. "Anisotropic transport and quantum oscillations in the quasi-one-dimensional TaNiTe<sub>5</sub>: Evidence for the nontrivial band topology." *The Journal of Physical Chemistry Letters* 11.18 (2020): 7782-7789.
- [2] Yaji, Koichiro, et al. "High-resolution three-dimensional spin-and angle-resolved photoelectron spectrometer using vacuum ultraviolet laser light." *Review of Scientific Instruments* 87.5 (2016): 053111.
- [3] Kresse, Georg, and Jürgen Furthmüller. "Efficiency of ab-initio total energy calculations for metals and semiconductors using a plane-wave basis set." *Computational materials science* 6.1 (1996): 15-50.
- [4] Wu, QuanSheng, et al. "WannierTools: An open-source software package for novel topological materials." *Computer Physics Communications* 224 (2018): 405-416.